Journal of Photochemistry and Photobiology A: Chemistry 219 (2011) 32–41

Contents lists available at ScienceDirect

Journal of Photochemistry and Photobiology A: Chemistry

journal homepage: www.elsevier.com/locate/jphotochem

Photoinduced electron transfer in wild type and mutated flavodoxin from *Desulfovibrio vulgaris*, strain Miyazaki F.: Energy gap law

Kiattisak Lugsanangarm[a], Somsak Pianwanit[a], Sirirat Kokpol[a,*], Fumio Tanaka[b,**], Haik Chosrowjan[c], Seiji Taniguchi[c], Noboru Mataga[c]

[a] Department of Chemistry, Faculty of Science, Chulalongkorn University, Bangkok 10330, Thailand
[b] Department of Biochemistry, Center for Excellence in Protein Structure and Function, Faculty of Science, Mahidol University, Bangkok 10400, Thailand
[c] Division of Laser BioScience, Institute for Laser Technology, Utsubo-Honmachi, 1-8-4, Nishiku, Osaka 550-0004, Japan

ARTICLE INFO

Article history:
Received 13 September 2010
Received in revised form 10 January 2011
Accepted 21 January 2011
Available online 1 February 2011

Key words:
Flavodoxin
Photoinduced electron transfer
Molecular dynamic simulation
Kakitani and Mataga theory
Energy gap law

ABSTRACT

Time–dependent changes in the geometrical factors near the isoalloxazine (Iso) residue of FMN in three mutant isoforms [Y97F, W59F and W59F–Y97F (DM, double mutation)] of the flavodoxin (FD) from *Desulfovibrio vulgaris*, strain Miyazaki F., were obtained by molecular dynamic (MD) simulation. The center to center distances from Iso to Trp59 in Y97F and to Tyr97 in W59F were 0.78 nm and 0.55 nm, respectively. The remarkable fluorescence quenching in these proteins has been explained in terms of photoinduced electron transfer (ET) from the Trp59 and/or Tyr97 residues to the excited isoalloxazine (Iso*). The ultrafast fluorescence dynamics of the wild type (WT) and the Y97F, W59F and DM variant FDs reported by Mataga et al. (J. Phys. Chem. B 106 (2002) 8917–8920), were simultaneously analyzed by the electron transfer theory of Kakitani and Mataga (KM theory) and the atomic coordinates determined by MD, according to a non-linear least squares method. Agreements between the observed and calculated decays were all very good. The obtained physical constants contained in the KM theory were, for Trp and Tyr, respectively, a frequency factor (ν_0) of 3.09×10^3 ps^{-1} and 2.46×10^3 ps^{-1}, an ET process coefficient (β) of 55.6 nm^{-1} and 9.64 nm^{-1}, a critical transfer distance (R_0) of 0.772 nm and 0.676 nm, plus a free energy related to the electron affinity of Iso* (G^0_{Iso}) of 7.67 eV. These constants were common to all three mutant FD systems. In contrast, the static dielectric constant depended on the FD systems, being 4.78, 4.04 and 2.28 in the Y97F, W59F and DM variant FDs, respectively. The mean ET rate to Iso* was fastest from Trp59 in Y97F among the three systems. The total free energy gap in the FD systems was obtained as a sum of the net electrostatic (*ES*) energy between ion pairs and the standard free energy gap. A plot of $\ln k_{ET}/\lambda_S$ vs. $-\Delta G^0_T/\lambda_S$ in all ET donors, where k_{ET} is ET rate, λ_S is the reorganization energy and ΔG^0_T is the total free energy gap, revealed that $\ln k_{ET}/\lambda_S$ can be expressed by a parabolic function of $-\Delta G^0_T/\lambda_S$ and the ET process in FD took place mostly in the normal region.

1. Introduction

The electron transfer phenomena in proteins are of importance in the fields of physics, chemistry and biology [1–3]. Photoinduced electron transfer (ET) plays an essential role in photosynthetic systems and photoreceptors in plants and microorganisms. In the last decade a number of new flavin photoreceptors have been found [4–23]. In these BLUF (blue-light using flavin) units of the flavin photoreceptors, Trp and/or Tyr residues exist near isoalloxazine (Iso), and ET from Tyr to the excited isoalloxazine (Iso*) is considered to be the first step of the bacterial photoregulation of photosynthesis. DNA photolyase and cryptochrome also contain flavins [24]. Femtosecond dynamics of DNA photolyase has been investigated by a transient absorption spectroscopy [25,26].

Most flavoproteins other than flavin photoreceptors contain the aromatic amino acids Trp and Tyr near the Iso residue. These flavoproteins are practically non-fluorescent, but they emit fluorescence with a very short lifetime upon excitation with a sub-picosecond light pulse [27–33]. This remarkable fluorescence quenching is ascribed to ultrafast ET from the Trp and/or Tyr residues to the Iso* [34–37]. Since the seminal work on electron transfer theory by Marcus [1,38,39], many researchers have further developed the theory of ET [40–45]. However, these theories have been modeled for ET in bulk solution. It is not clear whether they are applicable to

* Corresponding author at: Department of Chemistry, Faculty of Science, Chulalongkorn University, Bangkok 10330, Thailand.
Tel.: +6622187583; fax: +6622187598.
** Corresponding author at. Department of Biochemistry,Center for Excellence in Protein Structure and Function, Faculty of Science, Mahidol University, Bangkok 10400, Thailand.
E-mail addresses: siriratkokpol@gmail.com (S. Kokpol), fukoh2003@yahoo.com (F. Tanaka).

1010-6030/$ – see front matter © 2011 Elsevier B.V. All rights reserved.
doi:10.1016/j.jphotochem.2011.01.013

ET in proteins, where a reliable method to quantitatively analyze ET in proteins is still required.

In the previously work, the differences in the fluorescence lifetimes between Y97F and W59F were elucidated by means of ET donor–acceptor distances of a static FD structure via X-ray crystallography[46] from *Desulfovibrio vulgaris*, Hildenborough [28]. However, we cannot obtain a non-exponential decay of the flavoproteins by this method. Accordingly, we believe that the dynamic analysis with dynamic structures is more reliable for ET rate and the understanding of fluorescence dynamics. Therefore, we have developed the method to analyze ET in proteins by using the atomic coordinates determined by MD simulations, Kakitani and Mataga (KM) theory, and experimental fluorescence dynamics [47–50]. By using this approach for FMN binding protein (FBP) and AppA, the following conclusions on ET in flavoproteins have been derived: (1) a non-exponential decay can be reproduced when the time over (MD time) which the simulation is run exceeds the experimental decay time; (2) the electrostatic (*ES*) energy between the ionic ET products and other ionic amino acids are influential upon the ET rates; (3) Trp and Tyr as ET donors have different ET parameters in KM theory as standard free energy gap (ΔG_0), frequency factor (ν_0), ET process coefficient (β) and critical distance (R_0), which will be described later; and (4) the static dielectric constant depends on the protein systems, which should be the local dielectric constant near the ion pair. However, these characteristics of ET in proteins were obtained from only a few flavoprotein systems and so it is very important to apply the present method for many more flavoproteins, in order to test its general applicability and usefulness.

Here, the ultrafast fluorescence dynamics of WT (wild type), Y97F (Tyr97 is replaced by Phe), W59F (Trp59 is replaced by Phe) and DM (double mutation, both of Trp59 and Tyr97 are replaced by Phe) flavodoxin (FD) systems are analyzed simultaneously to obtain a precise feature of the ET mechanism in FD, and to further verify the validity of the method. The mechanism of ET in FD was compared to those in FBP [47,48] and the flavin photoreceptor of AppA [49,50].

2. Methods of analyses

2.1. Protein structures and dynamic of the WT, Y97F, W59F and DM variant FDs

X-ray crystallography and or NMR based determination of the structure of FD is not available yet and so the structure of these systems were approximated by a homology modeling technique (unpublished work). In the present work, all systems are calculated for 5 ns. We found that all systems reached equilibrium, by RMSD analysis, after 3 ns as shown in Fig. S1 (Supplemental Material B). Therefore, we collected MD coordinate for analysis from 3 to 5 ns (net 2 ns).

2.2. ET theory

KM theory was used for the analyses, because it explains the distance-dependent average ET rates of flavoproteins [31] and the fluorescence decays of FBP very well [47]. The ET rate by KM theory [43–45] is expressed by Eq. (1);

$$k_{\mathrm{j}}^{\mathrm{i}}(t') = \frac{\nu_0^{\mathrm{q}}}{1+\exp\{\beta^{\mathrm{q}}(R_{\mathrm{j}}^{\mathrm{i}}-R_0^{\mathrm{q}})\}}\sqrt{\frac{k_{\mathrm{B}}T}{4\pi\lambda_{\mathrm{j}}^{\mathrm{i}}(t')}} \times \exp\left[-\frac{\{\Delta G_{\mathrm{q}}^0 - e^2/\varepsilon_0^{\mathrm{j}}R_{\mathrm{j}}^{\mathrm{i}}(t') + \lambda_{\mathrm{j}}^{\mathrm{i}}(t') + ES_{\mathrm{j}}^{\mathrm{i}}(t')\}^2}{4\lambda_{\mathrm{j}}^{\mathrm{i}}(t')k_{\mathrm{B}}T}\right] \quad (1)$$

where i is the donating aromatic amino acid in the ET, such as Trp59, Tyr97, Tyr99 and Trp16, j denotes the FD system as WT, Y97F, W59F or DM variants and *q* denotes Trp or Tyr. In Eq. (1), time-dependent variables, $R_{\mathrm{j}}^{\mathrm{i}}(t')$, $\lambda_{\mathrm{j}}^{\mathrm{i}}(t')$ and $ES_{\mathrm{j}}^{\mathrm{i}}(t')$, where t' is MD time, are explicitly indicated, but (t') parts of these variables were omitted in text. ν_0^{q} is an adiabatic frequency of Trp or Tyr, β^{q} is a coefficient of the ET process for Trp or Tyr. R_0^{q} is a critical donor–acceptor distance between adiabatic and non-adiabatic ET. $R_{\mathrm{j}}^{\mathrm{i}}$ is the distance between the Iso and the donor amino acid i in the FD system j, expressed as a center to center (R_{c}) distance. The ET process is adiabatic when $R_{\mathrm{j}}^{\mathrm{i}} < R_0^{\mathrm{q}}$, and non-adiabatic when $R_{\mathrm{j}}^{\mathrm{i}} > R_0^{\mathrm{q}}$. $ES_{\mathrm{j}}^{\mathrm{i}}$ is the net *ES* energy between the Iso anion or a donor cation and all other ionic groups in the FD system j, which will be described later. $\varepsilon_0^{\mathrm{j}}$ is a static dielectric constant of the FD system j. k_{B}, T and e are the Boltzmann constant, temperature and electron charge, respectively.

$\lambda_{\mathrm{j}}^{\mathrm{i}}$ is the solvent reorganization energy [31] of a donor i in the FD system j and is expressed in Eq. (2);

$$\lambda_{\mathrm{j}}^{\mathrm{i}} = e^2\left(\frac{1}{2a_1}+\frac{1}{2a_2}-\frac{1}{R_{\mathrm{j}}^{\mathrm{i}}}\right)\left(\frac{1}{\varepsilon_\infty}-\frac{1}{\varepsilon_0^{\mathrm{j}}}\right) \quad (2)$$

where a_1 and a_2 are the radii of the acceptor and donor, assuming these reactants are spherical. The optical dielectric constant (ε_∞) used was 2.0. The radii of Iso, Trp and Tyr were determined in the following way. (1) The three dimensional sizes of lumiflavin for Iso, 3-methylindole for Trp, and *p*-methylphenol for Tyr were obtained by the semi-empirical molecular orbital method (PM3). (2) The volumes of these molecules were determined as asymmetric rotors. (3) Radii of the spheres having the same volumes of the asymmetric rotors were obtained. The value of a_1 of Iso was 0.224 nm, and those of a_2 for Trp and Tyr were 0.196 nm and 0.173 nm, respectively.

The standard free energy change was expressed with the ionization potential of the ET donor, $E_{\mathrm{q}}^{\mathrm{IP}}$, as in Eq. (3);

$$\Delta G_{\mathrm{q}}^0 = E_{\mathrm{q}}^{\mathrm{IP}} - G_{\mathrm{Iso}}^0 \quad (3)$$

where G_{Iso}^0 is the standard Gibbs energy related to electron affinity of Iso*. The $E_{\mathrm{q}}^{\mathrm{IP}}$ values for Trp and Tyr were 7.2 and 8.0 eV, respectively, used in this analysis.

2.3. ES energy in the proteins

Protein systems contain many ionic groups, which may influence the ET rate. The *ES* energy between all ionic groups in the FD system j, including the phosphate anions of FMN, and Iso anion [ES_{j}(Iso)], Trp59$^+$ [ES_{j}(Trp59)], Tyr97$^+$ [ES_{j}(Tyr97)], Tyr99$^+$ [ES_{j}(Tyr99)] and Trp16$^+$ [ES_{j}(Trp16)], are expressed by Eq. (4), respectively. FD contains 12 Glu, 15 Asps, 12 Lyss and 8 Args residues plus two negative charges at the FMN phosphate.

$$ES_{\mathrm{j}}(\mathrm{w}) = \sum_{i=1}^{12}\frac{C_{\mathrm{w}}\cdot C_{\mathrm{Glu}}}{\varepsilon_0^{\mathrm{j}}R_{\mathrm{j}}^{\mathrm{w}}(\mathrm{Glu}\text{-}i)} + \sum_{i=1}^{15}\frac{C_{\mathrm{w}}\cdot C_{\mathrm{Asp}}}{\varepsilon_0^{\mathrm{j}}R_{\mathrm{j}}^{\mathrm{w}}(\mathrm{Asp}\text{-}i)} + \sum_{i=1}^{2}\frac{C_{\mathrm{w}}\cdot C_{\mathrm{Lys}}}{\varepsilon_0^{\mathrm{j}}R_{\mathrm{j}}^{\mathrm{w}}(\mathrm{Lys}\text{-}i)} + \sum_{i=1}^{8}\frac{C_{\mathrm{w}}\cdot C_{\mathrm{Arg}}}{\varepsilon_0^{\mathrm{j}}R_{\mathrm{j}}^{\mathrm{w}}(\mathrm{Arg}\text{-}i)} + \sum_{i=1}^{2}\frac{C_{\mathrm{w}}\cdot C_{\mathrm{P}}}{\varepsilon_0^{\mathrm{j}}R_{\mathrm{j}}^{\mathrm{w}}(\mathrm{P}\text{-}i)} \quad (4)$$

In Eq. (4), any of Iso, Trp59, Tyr97, Trp16 and Tyr99 were represented by w. C_{Iso} is the charge of the Iso anion and is equal to $-e$. C_{Trp59}, C_{Tyr97}, C_{Trp16} and C_{Tyr99} are the charges of the Trp59, Tyr97, Trp16 and Tyr99 cations, respectively, and are all equal to $+e$. C_{Glu} and C_{Asp} are the charges of the Glu and Asp anions, respectively, and are equal to $-e$. C_{Lys} and C_{Arg} are the charges of the Lys and Arg cations, respectively, and are equal to $+e$. C_{P} is the charge of the FMN phosphate and is equal to $-e$. We assumed that these groups are all in an ionic state in solution since the fluorescence dynamics

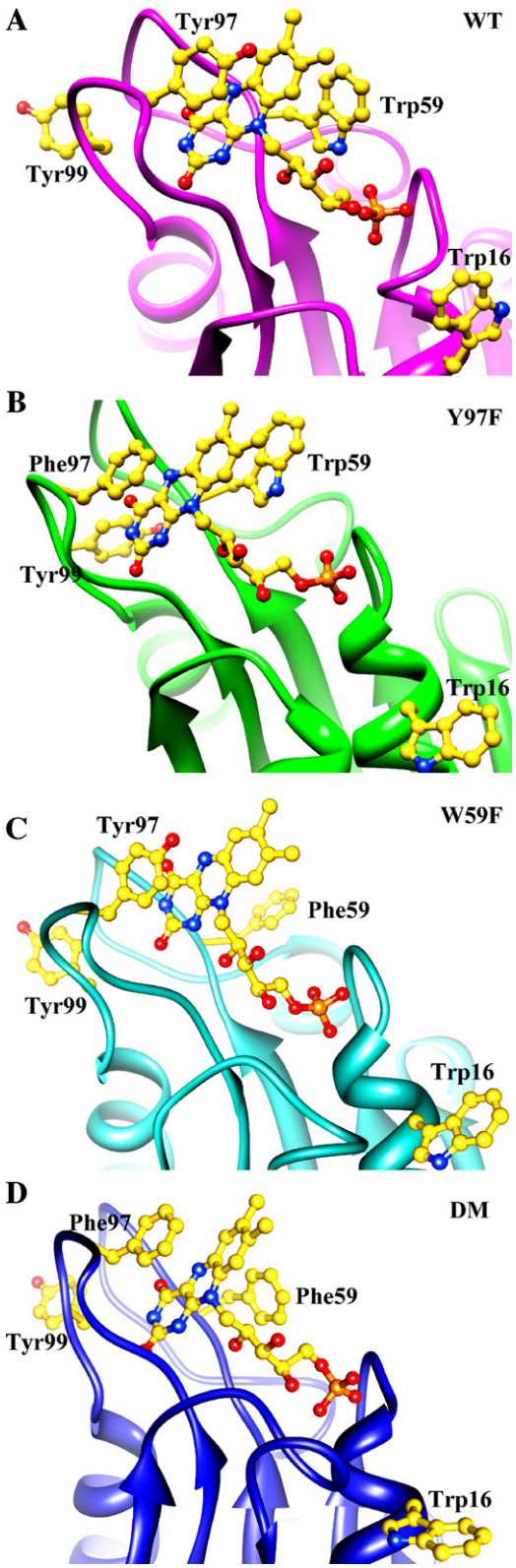

Fig. 1. Comparison of the protein structures among the WT and the Y97F, W59F and DM FD variants. (A) WT, (B) Y97F, (C) W59F and (D) DM. These structures were determined by homology modeling using the X-ray structure of flavodoxin *Desulfovibrio vulgaris*, strain Hildenborough (PDB code: 1J8Q) as the template.

Table 1
Geometrical factors relative to Iso in the mutated FD systems obtained by MD.[a]

Geometrical factor	Y97F			W59F			DM			WT[b]			
	Trp59	Tyr99	Trp16	Tyr97	Tyr99	Trp16	Tyr99	Trp16	Tyr97	Trp59	Tyr97	Tyr99	Trp16
Rc^{c} (nm)	0.78 ± 0.0001	1.04 ± 0.0002	2.12 ± 0.0003	0.55 ± 0.0001	1.36 ± 0.0005	1.82 ± 0.0004	1.35 ± 0.0005	2.02 ± 0.0005	0.64 ± 0.0010	0.54 ± 0.0009	1.28 ± 0.0024	1.72 ± 0.0053	
Re^{d} (nm)	0.26 ± 0.0002	0.34 ± 0.0005	1.54 ± 0.0004	0.30 ± 0.0001	0.54 ± 0.0004	1.39 ± 0.0004	0.496 ± 0.0005	1.44 ± 0.0005	0.25 ± 0.0015	0.30 ± 0.0015	0.53 ± 0.0026	1.18 ± 0.0045	
Inter-planar angle (°)	31.2 ± 0.13	61.3 ± 0.25	53.7 ± 0.22	18.6 ± 0.07	36.4 ± 0.08	−20.8 ± 0.08	−28.6 ± 0.09	30.9 ± 0.14	−42.8 ± 0.05	14.0 ± 0.05	23.5 ± 0.07	−18.1 ± 0.06	

[a] Mean ± SE. The means values were obtained taking an average over MD time (2 ns) with 0.1 ps time intervals. The distances and inter-planar angles are shown between Iso and the aromatic amino acids.
[b] Data were taken from Ref. [51].
[c] Center to center distance between Iso and the aromatic amino acids.
[d] Edge to edge distance.

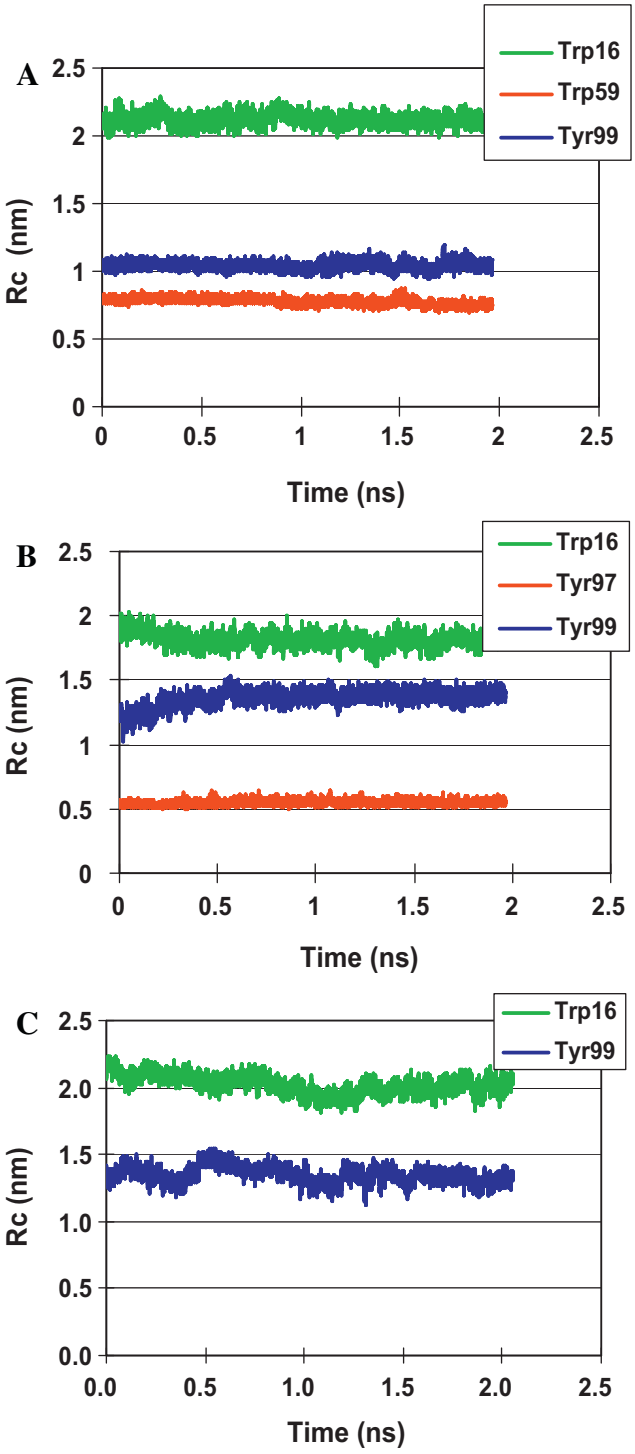

Fig. 2. Time-dependent changes in R_c between Iso and the aromatic amino acids. (A) Y97F, (B) W59F and (C) DM. Tyr97, Trp59, etc. in the inserts denote the distances between Iso and Tyr97, between Iso and Trp59, etc., respectively.

of the FD systems were measured in buffer solutions at pH 8. The distances between the chromophore w and *i*th Glu (i = 1–12) in the FD system j are denoted as R_j^w(Glu-i). Here, *ES* energies were evaluated using only the ionic groups in the proteins. When *ES* energies were obtained with partial charge densities of all the atoms in the proteins, they did not differ much from those obtained with the present method [51].

Net *ES* energies of the donor w in FD j are expressed as follows:

$$\text{For } k_j^i(t'), \quad ES_j{}^i = ES_j(\text{Iso}) + ES_j(\text{i}) \tag{5}$$

Here i represents Trp59, Tyr97, Trp16 and Tyr99 in the FD system j, respectively.

The values of *ES* energy, as given by Eq. (4), and, consequently, those for ES_j^i, as given by Eq. (5), were separately evaluated among the WT, Y97F, W59F and DM FD variants, because the distances between the Iso anion and the ionic groups, and between the cations and ionic groups, were different among these four systems.

2.4. Calculation of fluorescence decays

The observed fluorescence decays [28] of the WT, Y97F, W59F and DM systems are expressed by Eqs. (6)–(9), respectively.

$$F_{obs}^{WT}(t) = \exp\left(\frac{-t}{\tau_1^{WT}}\right) \tag{6}$$

$$F_{obs}^{Y97F}(t) = \alpha_1^{Y97F}\ \exp\left(\frac{-t}{\tau_1^{Y97F}}\right) + \alpha_2^{Y97F}\exp\left(\frac{-t}{\tau_2^{Y97F}}\right) \tag{7}$$

$$F_{obs}^{W59F}(t) = \alpha_1^{W59F}\ \exp\left(\frac{-t}{\tau_1^{W59F}}\right) + \alpha_2^{W59F}\exp\left(\frac{-t}{\tau_2^{W59F}}\right) \tag{8}$$

$$F_{obs}^{DM}(t) = \exp\left(\frac{-t}{\tau_1^{DM}}\right) \tag{9}$$

Here $\tau_1^{WT} = 0.157$ ps, $\tau_1^{Y97F} = 0.245$ ps ($\alpha_1^{Y97F} = 0.85$), $\tau_2^{Y97F} = 4.0$ ps ($\alpha_2^{W59F} = 0.15$), $\tau_1^{W59F} = 0.322$ ps ($\alpha_1^{W59F} = 0.83$), $\tau_2^{W59F} = 5.5$ ps ($\alpha_2^{W59F} = 0.17$), $\tau_1^{DM} = 18$ ps. The calculated fluorescence decays of the WT and the Y97F, W59F and DM FD variants are expressed by Eqs. (10)–(13), respectively;

$$F_{calc}^{WT}(t) = \langle \exp[-\{k_{WT}^{Trp59}(t') + k_{WT}^{Tyr97}(t') + k_{WT}^{Tyr99}(t') + k_{WT}^{Trp16}(t')\}t]\rangle_{AV} \tag{10}$$

$$F_{calc}^{Y97F}(t) = \langle \exp[-\{k_{Y97F}^{Trp59}(t') + k_{Y97F}^{Tyr99}(t') + k_{Y97F}^{Trp16}(t')\}t]\rangle_{AV} \tag{11}$$

$$F_{calc}^{W59F}(t) = \langle \exp[-\{k_{W59F}^{Tyr97}(t') + k_{W59F}^{Tyr99}(t') + k_{W59F}^{Trp16}(t')\}t]\rangle_{AV} \tag{12}$$

$$F_{calc}^{DM}(t) = \langle \exp[-\{k_{DM}^{Tyr99}(t') + k_{DM}^{Trp16}(t')\}t]\rangle_{AV} \tag{13}$$

where $k_{WT}^{Trp59}(t')$, $k_{Y97F}^{Trp59}(t')$, $k_{W59F}^{Tyr97}(t')$ and so on, in the calculated decays, represent the ET rates of Trp59 in WT, Trp59 in Y97F, Tyr97 in W59F, and so on, respectively. These ET rates are dependent on MD simulation time t' as shown in Eq. (1). In Eqs. (10)–(13), t' denotes MD time (0–2 ns), whilst t is fluorescence decay time (0–2 ps).

Fluorescence decays were calculated up to 2 ps with time intervals of 0.002 ps, since the decays were measured in this time range [28]. $\langle\cdots\rangle_{AV}$ represents the averaging procedure of the exponential function in Eqs. (10)–(13) over t' up to 2 ns with 0.1 ps time intervals. In Eqs. (10)–(13) we have assumed that the decay functions during the MD time ranges can always be expressed by exponential functions at every instant of time, t'. The present method is mathematically equivalent to the one by Henry and Hochstrasser [52], when the time range (2 ns) of MD data is much longer than one (2 ps) of fluorescence data, as described in the Supplemental Material A.

2.5. Determination of ET parameters

The unknown ET parameters (ν_0^{Trp}, ν_0^{Tyr}, β^{Trp}, β^{Tyr}, R_0^{Trp}, R_0^{Tyr}, ε_0^{WT}, ε_0^{Y97F}, ε_0^{W59F}, ε_0^{DM} and G_{Iso}^0) contained in the KM theory (see Eq. (1))

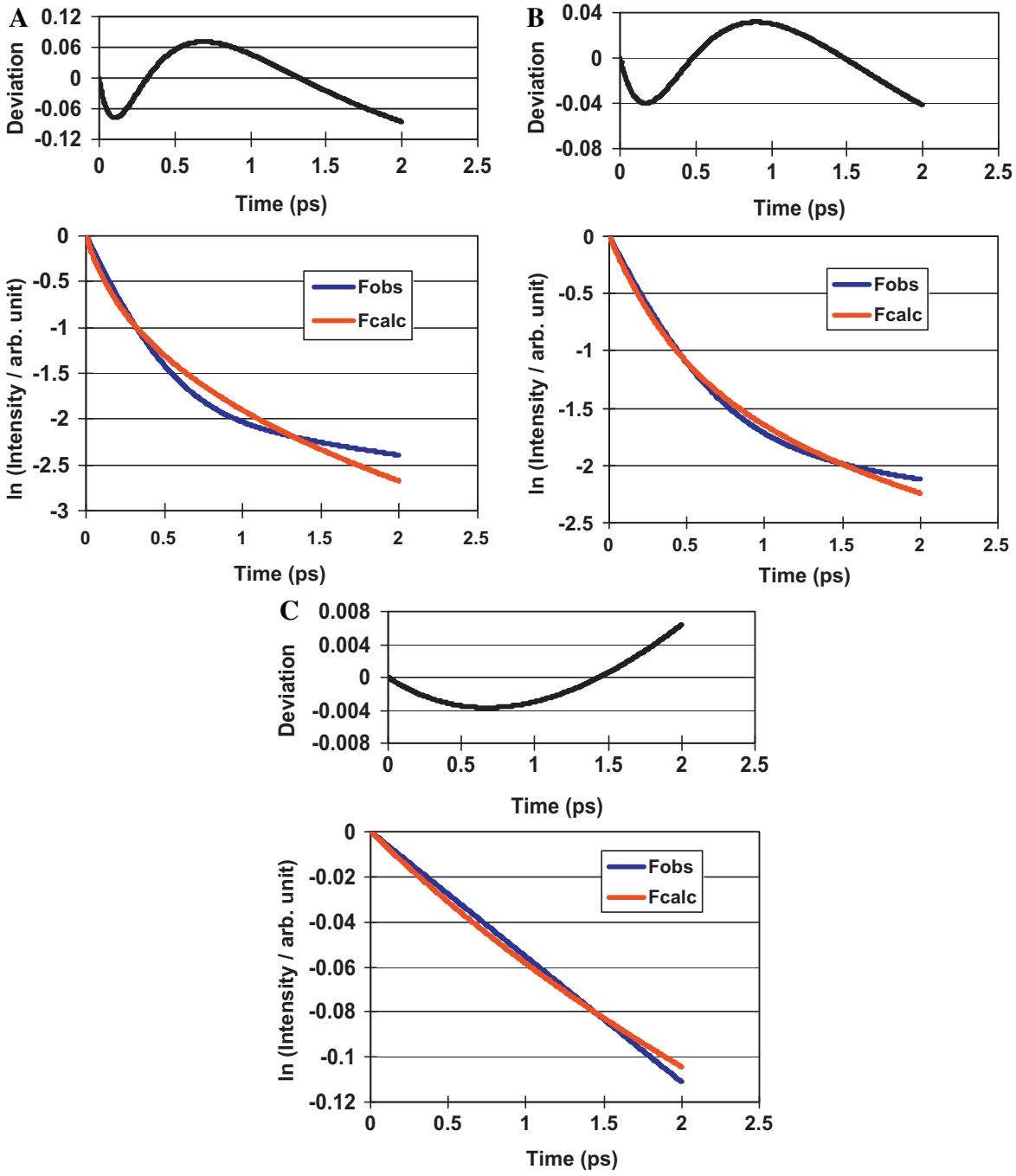

Fig. 3. Fluorescence decays of the Y97F, W59F and DM FD variants. (A) Y97F, (B) W59F and (C) DM. Upper panels in A–C represent deviations between the observed (Fobs) and calculated (Fcalc) fluorescence decays. Obtained ET parameters are listed in Table 2.

were determined so as to obtain the minimum value of χ^2, defined by Eq. (14), by means of a non-linear least squares method, according to the Marquardt algorithm, as previously reported [47–50].

$$\chi^2 = \frac{1}{N_{WT}}\sum_{i=1}^{N_{WT}}\frac{\{F_{calc}^{WT}(t_i) - F_{obs}^{WT}(t_i)\}^2}{F_{calc}^{WT}(t_i)} + \frac{1}{N_{Y97F}}\sum_{i=1}^{N_{Y97F}}\frac{\{F_{calc}^{Y97F}(t_i) - F_{obs}^{Y97F}(t_i)\}^2}{F_{calc}^{Y97F}(t_i)} + \frac{1}{N_{W59F}}\sum_{i=1}^{N_{W59F}}\frac{\{F_{calc}^{W59F}(t_i) - F_{obs}^{W59F}(t_i)\}^2}{F_{calc}^{W59F}(t_i)} + \frac{1}{N_{DM}}\sum_{i=1}^{N_{DM}}\frac{\{F_{calc}^{DM}(t_i) - F_{obs}^{DM}(t_i)\}^2}{F_{calc}^{DM}(t_i)} \quad (14)$$

where N_{WT}, N_{Y97F}, N_{W59F} and N_{DM} denote the number of time intervals of the fluorescence decays of the WT and the Y97F, W59F and DM FD variants, respectively, and were all 1000. Deviations of the four FD systems between the observed and calculated intensities

Table 2
The best-fit ET parameters.[a]

System		ν_0^{q}[b] (ps^{-1})		β^{q}[b] (nm^{-1})		R_0^{q}[b] (nm)		G_{Iso}^{0}[b] (eV)	ε_0^{j}[b]	χ^2[c]
		Trp	Tyr	Trp	Tyr	Trp	Tyr			
FD	Y97F	3090	2460	55.6	9.64	0.772	0.676	7.67	4.78	2.61×10^{-3}
	W59F								4.04	5.97×10^{-4}
	DM								2.28	3.04×10^{-5}
	WT[d]								5.85	5.90×10^{-4}
AppA[e]	WT	2304	2661	18.1	6.25	0.539	2.74	8.53	29.0	4.60×10^{-4}
	Y21F								13.7	3.08×10^{-4}
	W104F								2.45	1.60×10^{-4}
FBP[f]	WT, W32Y, W32A	1016	197	21.0	6.64	0.570	0.0	8.97	9.86	5.24×10^{-4}

[a] ν_0^{q}, β^{q}, R_0^{q} (q = Trp or Tyr) were common for the three mutated FD systems and the WT. ε_0^{j} depended on FD species j. These values were determined from the fluorescence dynamics of the WT and variant FDs by means of the best-fit procedure, as described in the text.
[b] ΔG_q^0 in Eq. (1) is obtained by Eq. (3) with G_{Iso}^0. The values of ΔG_q^0 were −0.467 eV for Trp and 0.333 eV for Tyr.
[c] χ^2 was evaluated independently for each system. Total value of χ^2 was 5.55×10^{-4}.
[d] Data from Ref. [51].
[e] Data from Refs. [49,50].
[f] Data from Ref. [48]. Three fluorescence decays of WT, W32Y and W32A FMN binding proteins were analyzed with common dielectric constant.

are defined by Eq. (15);

$$Deviation(\mathrm{j}; t_i) = \frac{\{F_{calc}^{j}(t_i) - F_{obs}^{j}(t_i)\}}{\sqrt{F_{calc}^{j}(t_i)}} \quad (15)$$

Here j = WT, W59F, Y97F and DM.

3. Results

3.1. Comparison of protein structures around Iso among the four FD systems

Typical protein structures of the WT and the Y97F, W59F and DM variant FDs, as determined by homology modeling and MD, are shown in Fig. 1. Time-dependent changes in the R_c between Iso and Tyr97, Trp59, Trp16 and Tyr99 are also shown in Fig. 2. The changes in the mean edge to edge distances (R_e) are shown in Fig. S2 (Supplemental Material B).

The mean R_c and R_e values are listed in Table 1. The mean value of R_c between Iso and Trp59 in Y97F (0.78 nm) was significantly longer than that (0.64 nm) in the WT FD. The values of R_c for Trp16 and Tyr99 were quite different among the mutated FD variants. Thus, the R_c of Trp16 was longest (2.12 nm) in the Y97F FD and shortest (1.72 nm) in the WT, whilst for Tyr99 it was longest (1.36 nm) in W59F and shortest (1.04 nm) in Y97F. However, the values of R_e for Trp59 in Y97F and for Tyr97 in W59F were almost identical with those for Trp59 and Tyr97 in the WT. The time-dependent changes in the inter-planar angles between Iso and Trp59, Trp16 and Tyr99 in Y97F are shown in Fig. S3 (Supplemental Material B). The time-dependent changes were remarkable in Tyr99 and Trp16. For Trp16, the angle carried from around 70° initially, increasing to 160° at 0.7 ns and then decreasing to 20° at 1.3 ns, whilst for Tyr99 it was initially around 50°, increased to 160° at 0.7 ns, decreased to 30° at 0.9 ns, and increased again to around 100°. The mean values of the angle are listed in Table 1. The angle between Iso and Trp59 varied considerably between Y97F (31°) and the WT (-43°), whilst the angles between Iso and Tyr97 were similar in these systems (19° and 14°, respectively). The time-dependent changes in the inter-planar angles in the W59F and DM variants are shown in Fig. S4 (Supplemental Material B). Contrary to that seen in Y97F, the angles rapidly fluctuate around constant values, except for Trp16 in the DM variant, which increased with time from 20° to 60°. The mean angle of Tyr97 in the W59F mutation did not differ much from that of the WT. The mean angles of Tyr99 were 61° in Y97F compared to −29° in the DM. The angles of Trp16 were 54° in Y97F, −21° in W59F and −18° in the WT FDs.

Table 3
Energy gap law of ET in FD.[a]

Physical quantity	WT				W59F			Y97F			DM	
	Trp59	Tyr97	Trp16	Tyr99	Tyr97	Trp16	Tyr99	Trp59	Trp16	Tyr99	Trp16	Tyr99
$\ln k_j^{i}$[b]	1.96	−6.68	−124.97	−114.99	1.14	−69.10	−155.82	1.60	−96.53	−139.87	−94.97	−2.60
λ_j^{i}[c] (eV)	1.53	1.54	1.99	2.06	1.20	1.54	1.59	1.47	1.81	1.74	0.377	0.385
ES energy[d] (eV)	−2.85	−2.93	−0.0993	−0.118	−3.82	−2.62	−0.176	−3.41	−2.21	−0.150	−4.67	−6.80
Net *ES* energy[e] (eV)	−0.0172	−0.0942	2.73	2.71	−0.219	0.984	3.42	−0.00159	1.20	3.26	2.13	0.0131
ΔG_q^{0}[f] (eV)	−0.467	0.333	−0.467	0.333	0.333	−0.467	0.333	−0.467	−0.467	0.333	−0.467	0.333
ES energy between donor and acceptor[g]	−0.384	−0.460	−0.144	−0.193	−0.652	−0.196	−0.263	−0.386	−0.142	−0.289	−0.313	−0.470
$-\Delta G_{ij}^{0}$[h] (eV)	0.868	0.221	−2.12	−2.86	0.583	−0.321	−3.49	0.855	−0.594	−3.31	−1.35	0.124
$-\Delta G_{ij}^{0}/\lambda_j^{i}$	0.569	0.143	−1.07	−1.39	0.450	−0.209	−2.19	0.583	−0.329	−1.90	−3.58	0.322
$(\ln k_j^{i})/\lambda_j^{i}$	1.28	−4.33	−62.84	−55.95	0.951	−44.95	−97.84	1.09	−53.46	−80.22	−251.93	−6.76

[a] ET rate is given by Eq. (1). Data of WT were taken from Ref. [51].
[b] k_j^{i} is expressed in unit of ps^{-1}.
[c] Reorganization energy is given by Eq. (2).
[d] *ES* energies are given by Eq. (4). *ES* energies of Iso were 2.83 eV in WT, 3.60 eV in W59F, 3.41 eV in Y97F and 6.82 eV in DM.
[e] Net *ES* energies are given by Eq. (5).
[f] ΔG_q^0 is given by Eq. (3).
[g] *ES* energy between donor and acceptor is given by $-e^2/\varepsilon_0^{j}R_j^{i}$ in Eq. (1).
[h] Total free energy gap is given by Eq. (16).

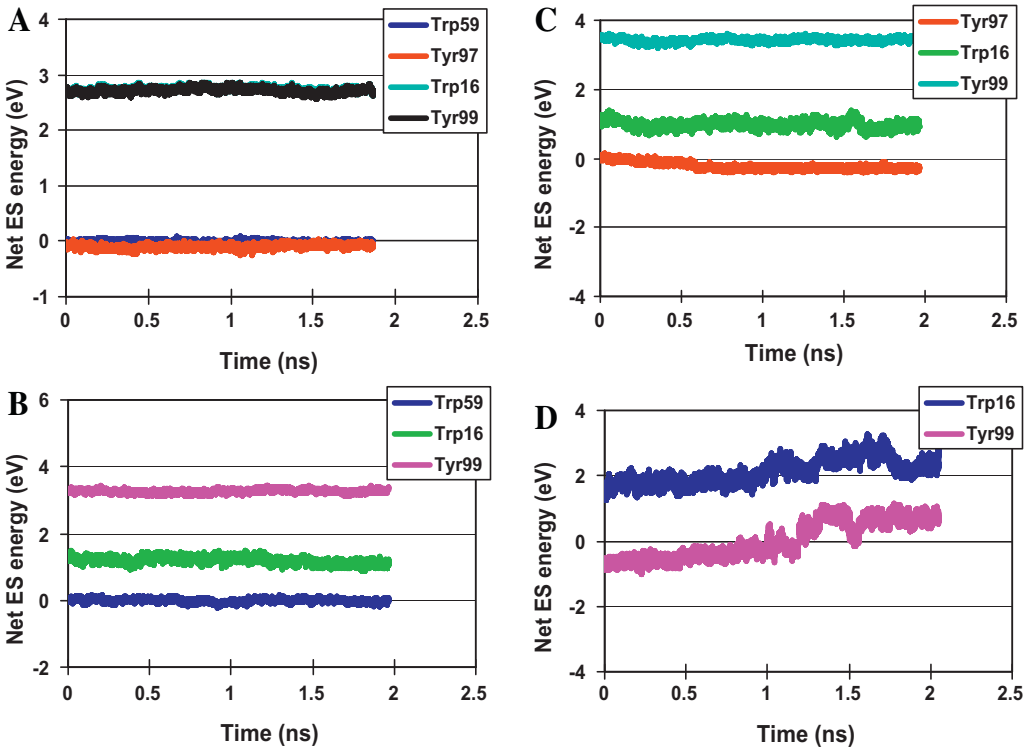

Fig. 4. Net *ES* energy in the WT and variant FDs. (A) WT, (B) Y97F, (C) W59F and (D) DM. Net *ES* energy means sum of *ES* energies of Iso and the aromatic amino acids. ET rate depends on net *ES* energy [see Eqs. (1) and (5)]. Trp59, Tyr97, Trp16 and Tyr99 in inserts denote net energies of Trp59, Tyr97, Trp16 and Tyr99, respectively.

3.2. Analyses of the fluorescence dynamics

Ultrafast fluorescence decays of the four FD systems were simultaneously analyzed with common ET parameters. Fig. 3 shows the observed and calculated fluorescence decays of the Y97F, W59F and DM variant FDs. The upper panels of the decay plots show the deviations between the observed and calculated decays. The decays of the WT [51] and the double mutated FD were single exponential, whereas those of the Y97F and W59F variant FDs were non-exponential. It is striking that two nearly single exponential and two double-exponential decay functions were reproduced with the same ET parameters (Table 2) of ν_0^q, β^q, R_0^q and ΔG_q^0 (q = Trp or Tyr), despite that all of fluorescence decay exponentially before taking average over MD time range. It is reasonable to assume that the dielectric constant near the ET donor and acceptor ions depends on the FD systems, because the polarity near the Iso* anion is different among the four FD systems.

If we consider that four decays were simultaneously analyzed with common parameters as ν_0^q, β^q and R_0^q (q = Trp or Tyr) and also the intensities are expressed in logarithm, agreements between the observed and calculated decays were satisfactory [the total value of χ^2 (5.55×10^{-4})] and acceptable as compared with our previous work, FMN binding protein systems [47].

3.3. ET parameters

The obtained ET parameters for the WT and the three mutant FD variants are listed in Table 2, along with those for the AppA and FBP taken from the literature for comparison. From these values, ΔG_q^0 was calculated by Eq. (3) to be −0.467 eV for Trp and 0.333 eV for Tyr. The adiabatic frequency (ν_0^q) of Trp in FD was ~1.3- and 3-fold greater than that for AppA and FBP, respectively, whilst the ν_0^q of Tyr in FD was 0.92- and 12.5-fold higher than that in AppA and FBP, respectively. The ET process coefficient (β^q) of Trp in FD was 3-fold and 2.6-fold greater than that in AppA and FBP, respectively, whilst the β^q of Tyr was 1.5-fold larger than that of both AppA and FBP. Finally, the R_0^q in FD was ca. 0.2 nm longer for Trp than that in AppA, but much shorter than that for the Tyr in AppA.

3.4. ES energies in the proteins

Fig. S5 (Supplemental Material B) shows the time-dependent changes in the *ES* energies of the Y97F, W59F and the DM FD variants, with the mean energies listed in Table 3 The mean energy [ES_j(Iso)] between the Iso anion and all other ionic groups was lowest in the WT and some 1.20-, 1.28- and 2.42-fold higher in the Y97F, W59F and DM FD variants, respectively. The mean energies of the Trp59 cation in Y97F, and the Tyr97 cation in W59F, were 1.20- and 1.30-fold lower, respectively, than those in the WT FD. For the Tyr99 and Trp16 cations, the mean energy was lower in all three FD variants than the WT, starting from slightly lower in Y97F up to the dramatically so in the double mutation.

For ET rates, the sum of the energies of Iso and ET donors (net energy) are important (see Eq. (5)). The time-dependent changes in the net *ES* energies (ES_j^i) are shown in Fig. 4. The mean net energy was −0.00159 eV for Trp59 in Y97F and −0.219 eV for Tyr97 in W59F, which were comparable to those in the WT at −0.0172 eV and −0.0942 eV, respectively. Fluctuations of these energies over time, i.e. time-dependent changes, may influence the non-exponential behavior of the fluorescence decay. *ES* energies from 5700 water molecules outside the protein and from partial charges of non-ionic amino acids in the protein were not evaluated here because they were relatively negligible with a contribution of less than 6% (to be submitted).

3.5. ET rates

ET rates were calculated with the best-fit ET parameters (see Table 2). Fig. 5 shows the ET rates in the three variant FDs (Y97F, W59F and DM). The ET rate was fastest from Trp59 to Iso* in Y97F,

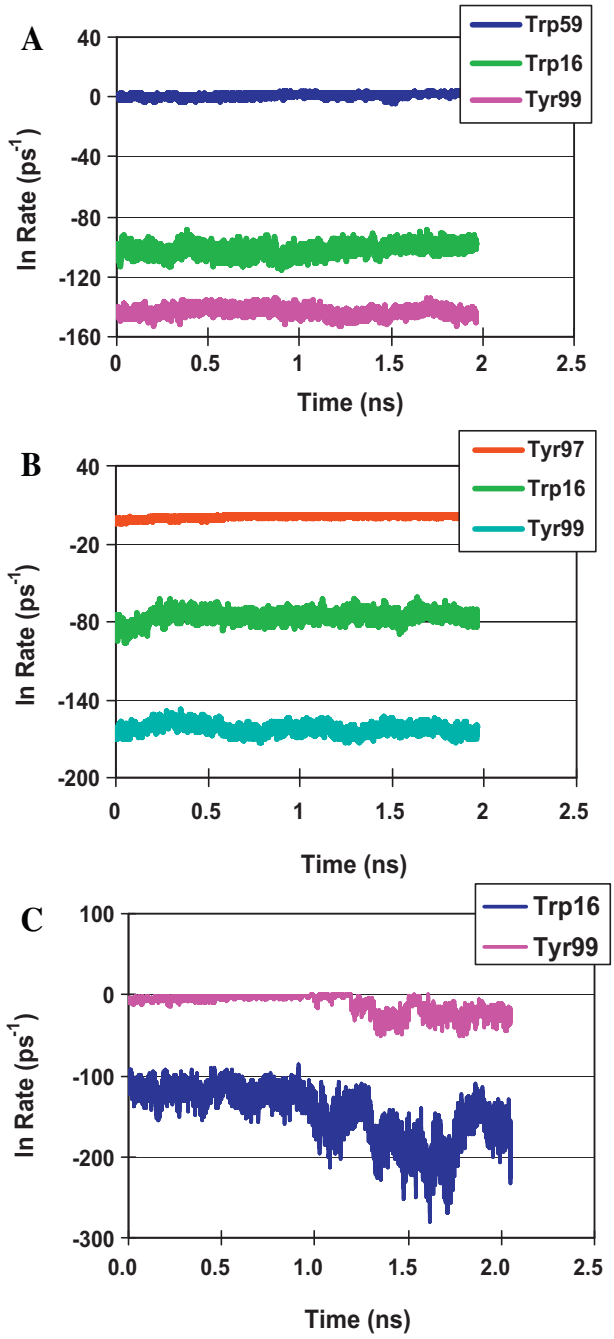

Fig. 5. ET rates in the mutated FD systems. (A) Y97F, (B) W59F and (C) DM. ET rates were calculated with the best-fit parameters listed in Table 2. Insert denotes ET donors.

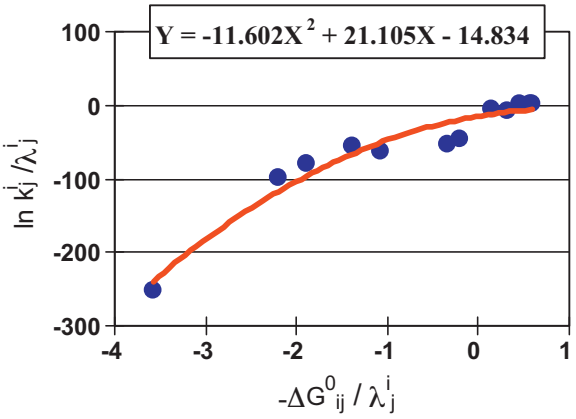

Fig. 6. Energy gap law of ET in FD. The ET rate is expressed in unit of ps^{-1}. Total free energy gap ($-\Delta G^0_{ij}$) is given by Eq. (16). Numerical data are listed in Table 3. ($\ln k^i_j$)/λ^i_j vs. $-\Delta G^0_{ij}/\lambda^i_j$ were plotted according to Eq. (17). Insert indicates an approximate parabolic function of the plot.

from Tyr97 in W59F and from Tyr99 in the DM. If Figs. 4 and 5 are compared, it is evident that the ET rate becomes slower with increasing levels of the net *ES* energy, which implies that the *ES* energy plays an important role in determining the ET rate. The mean values of the ET rates are listed in Table 3, where that from Trp59 to Iso* in Y97F (5.40 ps^{-1}) was slightly slower than that in the WT (7.11 ps^{-1}), whilst that from Tyr97 in W59F (3.18 ps^{-1}) was much faster than the corresponding value in the WT (1.26×10^{-3} ps^{-1}). It is noted that the ET rates from Tyr99 to Iso* were negligibly slow in the WT, Y97F and W59F FD variants, but became dramatically faster in DM.

4. Discussion

The observed fluorescence dynamics of the WT and the three mutated FD systems were simultaneously analyzed with common ET parameters. All fluorescence decays were satisfactorily reproduced with the best-fit ET parameters. The obtained ET parameters were compared with those of the flavin photoreceptor AppA [49,50], and also with those of FBP [47,48] (see Table 2). The values of ν_0^{Trp} and ν_0^{Tyr} in FD were 3090 and 2460 ps^{-1}, respectively, whilst they were 2304 and 2661 ps^{-1} for Trp and Tyr, respectively, in AppA. In both protein systems ν_0^{Tyr} was greater than ν_0^{Trp}, which is remarkably different from that of FBP.

ν_0^q is related to the electronic interaction energy between the donor and the acceptor. In AppA, the greater ν_0^q in Tyr was elucidated in terms of the hydrogen bond chain, Tyr21–Gln63–Iso* [49,50]. In FD, the R_c value between Iso and Tyr97 was very short (0.55 nm) compared to the R_c of Trp59, which may be the reason why ν_0^{Tyr} was greater than ν_0^{Trp}, whilst β^{Trp} and β^{Tyr} did not differ much compared to those of AppA. The value of R_0^{Trp} in FD was 0.772 nm, which is considerably longer than that in AppA (0.539 nm). However, the R_0^{Tyr} in AppA was remarkably longer than that in FD, and this may be due to the long chain of hydrogen bonds from Tyr21 to Iso* through Gln63 [50].

In FBP, the ε_0 used was common among the three systems of FBP, whilst different values of ε_0 were used in FD (this work) and in AppA [49,50]. Agreements between the observed and calculated fluorescence decays were greatly improved when the ε_0 values were changed with the protein system. Iso, in all FD systems, are partly exposed to the water layer (unpublished work). ε_0^j (j = WT, Y97F, W59F and DM) were somewhat lower than those found for AppA and FBP.

The ET rate from Trp59 to Iso* in Y97F was faster than that from Tyr97 to Iso* in W59F, despite the fact that the distance between Iso and Tyr97 in W59F was shorter than that between Iso and Trp59 in Y97F. A similar result was also found in the WT, and these results suggest that the donor–acceptor distance and ν_0^q are not always critically important to the ET rate in the proteins. As shown in Figs. 4 and 5, and also in Table 3, the ET rate became faster as the net *ES* energy (ES^i_j) was reduced, which reveals that the net *ES* energy is the most important factor in determining the ET rate in the proteins. Fig. 6 shows the relationship between the ln ET rate and the total free energy gap (ΔG^0_{ij}). ΔG^0_{ij} was obtained from Eq. (16) (see

Eq. (1)).

$$-\Delta G_{ij}^{0} = -\left(\Delta G_{q}^{0} - \frac{e^2}{\varepsilon_0^{j} R_j^{i}} + ES_j^{i}\right) \quad (16)$$

The numerical data of these physical quantities are listed in Table 3. In the present FD systems the solvent reorganization energy (λ_j^i) was found to vary from 0.385 (Tyr99 in DM) to 2.06 (Tyr99 in WT) with the ET donor (amount of variation 1.68 eV). On the other hand, the values of total free energy gap, ΔG_{ij}^0, varied from −3.49 eV (Tyr99 in W59F) to 0.868 eV (Trp59 in WT), in which the net *ES* energy varied from 3.42 eV to −0.219 eV for Tyr99 and Tyr97, respectively, in W59F (amount of variation 3.64 eV.) Since the change in ΔG_q^0 was at most 0.8 eV and further amount of variation in *ES* energy between ion pair of the donor and acceptor $-e^2/\varepsilon_0^j R_j^i$ in Eq. (16) was at most 0.51 eV (varied from −0.652 eV (Tyr97 in W59F) to −0.142 eV (Trp16 in Y97F)). It is considered that the net *ES* energy ES_j^i is most influential factor among the ET parameters. $(\ln k_j^i)/\lambda_j^i$ may be plotted against $-\Delta G_{ij}^0/\lambda_j^i$ when λ_S^{jk} appreciably varies, as Eq. (17).

$$\frac{\ln k_j^i}{\lambda_j^i} \propto \left(\frac{-\Delta G_{ij}^0}{\lambda_j^i} + 1\right)^2 \quad (17)$$

Pre-exponential factors in Eq. (1) may be almost constant upon the variation of $-\Delta G_{ij}^0/\lambda_j^i$. The value of $(\ln k_j^i)/\lambda_j^i$ was −252 at $-\Delta G_{ij}^0/\lambda_j^i$ (Trp16 in DM; see Fig. 6) equals −3.58, and increased with $-\Delta G_{ij}^0/\lambda_j^i$. The value of $(\ln k_j^i)/\lambda_j^i$ became maximum at around 6 of $-\Delta G_{ij}^0/\lambda_j^i$, and then decreased with $-\Delta G_{ij}^0/\lambda_j^i$. The solid curve in Fig. 6 was an approximate parabolic function, $Y = -11.602X^2 + 21.105X - 14.834$, where Y is $(\ln k_j^i)/\lambda_j^i$, and X is $-\Delta G_{ij}^0/\lambda_j^i$. The results reveal that ET in FD mostly takes place in the normal region.

A number of works have reported on the free energy gap law in bulk solutions [53–57], but rarely reported in proteins. The energy gap law was experimentally demonstrated in the ET processes in photosystem I and in the reaction center of the purple bacterium, *Rhodobacter sphaeroides*, by Iwaki et al., where the ET takes place in the normal regions [58]. Turro et al. [59] found that ET in a homologous series of RuII diimines with cytochrome (cyt) *c* in its oxidized and reduced forms takes place in both the inverted region and normal region. ET in FD in the present work took place in the normal region.

Relationship between ET process and electron transfer process in dark is worth of discussion. The donor–acceptor distance dependence on λ_S^{qj} and $-e^2/\varepsilon_0 R_j$ are common in both processes. *ES* energy of Iso anion and other ionic amino acids is also common between both electron transfer processes. Many flavoproteins are involved in electron transfer processes in dark. ET analyses of the flavoproteins could also help to understand the electron transfer in the ground state of Iso in the proteins.

Acknowledgments

This work was supported by the Royal Golden Jubilee Ph.D. Program (3.C.CU/50/S.1), from Chulalongkorn University and Thailand Research Fund (TRF). Thanks are also given to Computational Chemistry Unit Cell, Chulalongkorn University and National Electronics and Computer Technology Center (NECTEC) for computing facilities. Center of Excellence for Petroleum, Petrochemicals and Advanced Materials (NCE-PPAM) is acknowledged.

Appendix A. Supplementary data

Supplementary data associated with this article can be found, in the online version, at doi:10.1016/j.jphotochem.2011.01.013.

References

[1] R.A. Marcus, N. Sutin, Biochim. Biophys. Acta 811 (1985) 265–322.
[2] H.B. Gray, J.R. Winkler, Annu. Rev. Biochem. 65 (1996) 537–561.
[3] V. May, O. Kuhn, Charge and Energy Transfer Dynamics in Molecular Systems, Wiley-VCH, Verlag GmbH Co, Weinheim, 2004.
[4] S. Masuda, C.E. Bauer, Cell 110 (2002) 613–623.
[5] B.J. Kraft, S. Masuda, J. Kikuchi, V. Dragnea, G. Tollin, J.M. Zaleski, C.E. Bauer, Biochemistry 42 (2003) 6726–6734.
[6] S. Anderson, V. Dragnea, S. Masuda, J. Ybe, K. Moffat, C. Bauer, Biochemistry 44 (2005) 7998–8005.
[7] S. Masuda, K. Hasegawa, T. Ono, Biochemistry 44 (2005) 1215–1224.
[8] M. Gauden, S. Yeremenko, W. Laan, I.H.M. van Stokkum, J.A. Ihalainen, R. van Grondelle, K.J. Hellingwerf, J.T.M. Kennis, Biochemistry 44 (2005) 3653–3662.
[9] W. Laan, M. Gauden, S. Yeremenko, R. van Grondelle, J.T.M. Kennis, K.J. Hellingwerf, Biochemistry 45 (2006) 51–60.
[10] M. Gauden, I.H.M. van Stokkum, J.M. Key, D.C. Luhrs, R. Van Grondelle, P. Hegemann, J.T.M. Kennis, Proc. Natl. Acad. Sci. U. S. A. 103 (2006) 10895–10900.
[11] A. Jung, J. Reinstein, T. Domratcheva, R.L. Shoeman, I. Schlichting, J. Mol. Biol. 362 (2006) 717–732.
[12] K.C. Toh, I.H.M. van Stokkum, J. Hendriks, M.T.A. Alexandre, J.C. Arents, M.A. Perez, R. van Grondelle, K.J. Hellingwerf, J.T.M. Kennis, Biophys. J. 95 (2008) 312–321.
[13] T. Domratcheva, B.L. Grigorenko, I. Schlichting, A.V. Nemukhin, Biophys. J. 94 (2008) 3872–3879.
[14] H. Yuan, S. Anderson, S. Masuda, V. Dragnea, K. Moffat, C. Bauer, Biochemistry 45 (2006) 12687–12694.
[15] R. Takahashi, K. Okajima, H. Suzuki, H. Nakamura, M. Ikeuchi, T. Noguchi, Biochemistry 46 (2007) 6459–6467.
[16] C. Bonetti, T. Mathes, I.H.M. van Stokkum, K.M. Mullen, M.L. Groot, R. van Grondelle, P. Hegemann, J.T.M. Kennis, Biophys. J. 95 (2008) 4790–4802.
[17] Q. Wu, W.H. Ko, K.H. Gardner, Biochemistry 47 (2008) 10271–10280.
[18] H. Nagai, Y. Fukushima, K. Okajima, M. Ikeuchi, H. Mino, Biochemistry 47 (2008) 12574–12582.
[19] Y. Fukushima, Y. Murai, K. Okajima, M. Ikeuchi, S. Itoh, Biochemistry 47 (2007) 660–669.
[20] K. Sadeghian, M. Bocola, M. Schutz, Phys. Chem. Chem. Phys. 12 (2010) 8840–8846.
[21] M. Unno, S. Kikuchi, S. Masuda, Biophys. J. 98 (2010) 1949–1956.
[22] V. Dragnea, A.I. Arunkumar, H. Yuan, D.P. Giedroc, C.E. Bauer, Biochemistry 48 (2009) 9969–9979.
[23] A.L. Stelling, K.L. Ronayne, J. Nappa, P.J. Tonge, S.R. Meech, J. Am. Chem. Soc. 129 (2007) 15556–15564.
[24] K. Brettel, M. Byrdin, Curr. Opin. Struct. Biol. 20 (2010) 693–701.
[25] Y.-T. Kao, C. Tan, S.-H. Song, N. Öztürk, J. Li, L. Wang, A. Sancar, D. Zhong, J. Am. Chem. Soc. 130 (2008) 7695–7701.
[26] J. Brazard, A. Usman, F. Lacombat, C. Ley, M.M. Martin, P. Plaza, L. Mony, M. Heijde, G.r. Zabulon, C. Bowler, J. Am. Chem. Soc. 132 (2010) 4935–4945.
[27] N. Mataga, H. Chosrowjan, Y. Shibata, F. Tanaka, Y. Nishina, K. Shiga, J. Phys. Chem. B 104 (2000) 10667–10677.
[28] N. Mataga, H. Chosrowjan, S. Taniguchi, F. Tanaka, N. Kido, M. Kitamura, J. Phys. Chem. B 106 (2002) 8917–8920.
[29] F. Tanaka, N. Mataga, Trends Chem. Phys. 11 (2004) 59–74.
[30] F. Tanaka, H. Chosrowjan, S. Taniguchi, N. Mataga, K. Sato, Y. Nishina, K. Shiga, J. Phys. Chem. B 111 (2007) 5694–5699.
[31] F. Tanaka, R. Rujkorakarn, H. Chosrowjan, S. Taniguchi, N. Mataga, Chem. Phys. 348 (2008) 237–241.
[32] H. Chosrowjan, S. Taniguchi, N. Mataga, F. Tanaka, D. Todoroki, M. Kitamura, J. Phys. Chem. B 111 (2007) 8695–8697.
[33] H. Chosrowjan, S. Taniguchi, N. Mataga, F. Tanaka, D. Todoroki, M. Kitamura, Chem. Phys. Lett. 462 (2008) 121–124.
[34] A. Karen, N. Ikeda, N. Mataga, F. Tanaka, Photochem. Photobiol. 37 (1983) 495–502.
[35] A. Karen, M.T. Sawada, F. Tanaka, N. Mataga, Photochem. Photobiol. 45 (1987) 49–54.
[36] D.P. Zhong, A.H. Zewail, Proc. Natl. Acad. Sci. U. S. A. 98 (2001) 11867–11872.
[37] J. Pan, M. Byrdin, C. Aubert, A.P.M. Eker, K. Brettel, M.H. Vos, J. Phys. Chem. B 108 (2004) 10160–10167.
[38] R.A. Marcus, J. Chem. Phys. 24 (1956) 979–989.
[39] C.C. Moser, J.M. Keske, K. Warncke, R.S. Farid, P.L. Dutton, Nature 355 (1992) 796–802.
[40] M. Bixon, J. Jortner, J. Phys. Chem. 95 (1991) 1941–1944.
[41] M. Bixon, J. Jortner, J. Phys. Chem. 97 (1993) 13061–13066.
[42] M. Bixon, J. Jortner, J. Cortes, H. Heitele, M.E. Michelbeyerle, J. Phys. Chem. 98 (1994) 7289–7299.
[43] T. Kakitani, N. Mataga, J. Phys. Chem. 89 (1985) 8–10.
[44] T. Kakitani, A. Yoshimori, N. Mataga, J. Phys. Chem. 96 (1992) 5385–5392.

[45] T. Kakitani, N. Matsuda, A. Yoshimori, N. Mataga, Prog. React. Kinet. 20 (1995) 347–381.
[46] K.D. Watenpaugh, L.C. Sieker, L.H. Jensen, Proc. Natl. Acad. Sci. U. S. A. 70 (1973) 3857–3860.
[47] N. Nunthaboot, F. Tanaka, S. Kokpol, H. Chosrowjan, S. Taniguchi, N. Mataga, J. Photochem. Photobiol. A: Chem. 201 (2009) 191–196.
[48] N. Nunthaboot, F. Tanaka, S. Kokpol, H. Chosrowjan, S. Taniguchi, N. Mataga, J. Phys. Chem. B 112 (2008) 13121–13127.
[49] N. Nunthaboot, F. Tanaka, S. Kokpol, J. Photochem. Photobiol. A: Chem. 207 (2009) 274–281.
[50] N. Nunthaboot, F. Tanaka, S. Kokpol, J. Photochem. Photobiol. A: Chem. 209 (2010) 79–87.
[51] K. Lugsanangarm, S. Pianwanit, S. Kokpol, F. Tanaka, H. Chosrowjan, S. Taniguchi, N. Mataga, J. Photochem. Photobiol. A: Chem. 217 (2011) 333–340.
[52] E.R. Henry, R.M. Hochstrasser, Proc. Natl. Acad. Sci. U. S. A. 84 (1987) 6142–6146.
[53] A. Yoshimori, T. Kakitani, J. Phys. Soc. Jpn. 61 (1992) 2577–2592.
[54] J. Jortner, M. Bixon, J. Photochem. Photobiol. A: Chem. 82 (1994) 5–10.
[55] A.I. Burshtein, E. Krissinel, J. Phys. Chem. 100 (1996) 3005–3015.
[56] M. Tachiya, K. Seki, J. Phys. Chem. A 111 (2007) 9553–9559.
[57] N. Mataga, S. Taniguchi, H. Chosrowjan, A. Osuka, K. Kurotobi, Chem. Phys. Lett. 403 (2005) 163–168.
[58] M. Iwaki, S. Kumazaki, K. Yoshihara, T. Erabi, S. Itoh, J. Phys. Chem. 100 (1996) 10802–10809.
[59] C. Turro, J.M. Zaleski, Y.M. Karabatsos, D.G. Nocera, J. Am. Chem. Soc. 118 (1996) 6060–6067.